Int J Adv Manuf Technol (2017) 92:81–99
DOI 10.1007/s00170-017-0081-z

ORIGINAL ARTICLE

Material removal model of ultrasonic elliptical vibration-assisted chemical mechanical polishing for hard and brittle materials

Defu Liu[1] · **Riming Yan**[1] · **Tao Chen**[1]

Received: 29 September 2016 / Accepted: 16 January 2017 / Published online: 17 February 2017
© Springer-Verlag London 2017

Abstract The chemical mechanical polishing (CMP) is widely used to polish hard and brittle materials. However, it is difficult for conventional CMP to achieve high material removal rate (MRR) and high surface quality while polishing of hard and brittle materials such as monocrystalline silicon. Therefore, ultrasonic elliptical vibration (UEV) is employed to aid conventional CMP in our research, which combines the functions of conventional CMP and ultrasonic machining. In the ultrasonic elliptical vibration-aided chemical mechanical polishing (UEV-CMP) experimental setup developed by us, the workpiece attached on the ultrasonic vibrator can vibrate simultaneously in both horizontal and vertical directions during CMP. It is found that the ultrasonic elliptical vibration can effectively increase the MRR while maintaining surface quality in conventional CMP. The possible mechanism in UEV-CMP is firstly analyzed chemically to establish a reasonable material removal rate model. The effects of the ultrasonic elliptical vibration on the interaction among the abrasive particles, polishing pad, and workpiece are investigated to explain why the MRR of UEV-CMP is higher than that of the conventional CMP. A mathematic model, which includes polishing variables such as morphology and material properties of polishing pad; abrasive size; and material properties of particles, frequency, and amplitude of the ultrasonic vibration as well as polishing process parameters, is set up to interpret the increase in MRR for UEV-CMP. The results from the MRR model show that the ultrasonic elliptical vibration can improve material removal by increasing both the chemical reaction efficiency of polishing solution and mechanical impact efficiency of the abrasive particles on the workpiece surface and also by increasing vibration amplitude in vertical direction as the horizontal vibration contributes less towards the increment of MRR. Experiments are conducted for model verification, which should be that the experimental results agree well with model predictions.

Keywords Ultrasonic elliptical vibration (UEV) · Chemical mechanical polishing (CMP) · Material removal rate (MRR) · Hard and brittle materials

1 Introduction

Chemical mechanical polishing (CMP) is a popular process for smoothing and planarization of uniform surfaces by using a combination of chemical reactions and mechanical forces [1–2]. CMP is widely used for finishing of materials with great hardness, high wear resistance, and chemical inertness including silicon wafer [3], sapphire substrate [4], silica glass [5–6], gallium nitride (GaN) [7], and silicon carbide (SiC) [8], which are employed frequently in integrated optoelectronic and semiconductor devices. With the rapid development of integrated optoelectronic and semiconductor industries, higher polishing quality and machining efficiency of CMP are requested.

However, the present research results show that the conventional CMP technology is hard to obtain high material removal rate (MRR) and perfect finished surface at the same time due to the material's properties [9–10]. As a promising finishing technique for hard and brittle materials, ultrasonic vibration-assisted machining may enhance the machining efficiency and improve the surface integrity due to a fundamental alternation in process kinematics [11–12]. To acquire high

✉ Defu Liu
liudefu@csu.edu.cn

[1] College of Mechanical and Electrical Engineering, Central South University, Changsha, Hunan Province 410083, China

MRR and great polished surface quality simultaneously, ultrasonic vibration is introduced into chemical mechanical polishing process, which has been proven to be very useful in improving the polishing quality and efficiency for the hard-machining materials, such as sapphire substrate [13–14], copper substrate [15], monocrystalline silicon wafer [16], SiC [17], and fused silica [18].

Lu et al. [13–14] developed an ultrasonic flexural vibration-assisted chemical mechanical polishing (UFV-CMP) system to improve both MRR and surface quality of sapphire substrates. The MRR of UFV-CMP was 2.5 times larger than that of conventional CMP. The roughness and flatness of the sapphire surfaces polished by UFV-CMP were 0.83 Å and 0.12 μm, respectively, which were much better than that of conventional CMP. Tsai et al. [15] introduced an ultrasonic vibration-assisted chemical mechanical polishing (UV-CMP) method to finish copper substrates. It was found that material removal rate of the copper substrates increased by approximately 50–90% relative to that of conventional CMP, and the roughness of the substrate surfaces was also improved dramatically. Li et al. [16] applied ultrasonic traveling wave with the frequency of 27.99 kHz to the CMP of wafer. According to the large amounts of experiments on the chemical mechanical polishing assisted by ultrasonic vibration, it was found that morphologies of silicon wafers polished by UV-CMP were superior to that of conventional CMP. A novel model of UV-CMP for silicon wafer was proposed, which could be used to explain the experimental results. Li et al. [18] combined ultrasonic elliptical vibration with fixed abrasive polishing to finish fused silica substrates, which was devoted to the understanding of the increase of MRR in ultrasonic vibration-assisted, fixed-abrasive polishing. It was known from the physical model proposed in the paper that the material removal rate increase was contributed to the vertical vibration while horizontal vibration could hardly influence the material removal rate due to the difference from chemical bonding between coria and glass in conjunction with mechanical abrasion of glass.

Ultrasonic elliptical vibration-assisted chemical mechanical polishing (UEV-CMP) has been proven to be an efficient finishing process; however, at present, the effects of the ultrasonic vibration on the chemical mechanical polishing process are still being discussed on the basis of the experimental researches and the material removal mechanism [18–22]. Only few researching paper discussed the material removal rate model of ultrasonic vibration-assisted chemical mechanical polishing on hard and brittle materials, and there is no perfect theory to analyze the roles played by the ultrasonic elliptical vibration in the chemical mechanical polishing so far. In this paper, a kind of experimental setup for "ultrasonic elliptical vibration-assisted chemical mechanical polishing" is designed, which can make workpiece vibrate simultaneously in two orthogonal directions with the same ultrasonic frequency. To investigate the material removal mechanism of UEV-CMP, the experiments about the effects of ultrasonic vibration on chemical reaction occurred between polishing slurry and workpiece, and mechanical impact of abrasive particles is conducted, respectively. Numerous variables are involved in the material removal process, such as abrasive particles, polishing pressure, polishing slurry chemistry, polishing pad, and ultrasonic vibration characteristics. The modeling of the MRR is crucial to understand the complexity of CMP process, and considerable research efforts have concentrated on this topic. A novel material removal rate model is proposed, which includes most polishing process factors, such as the morphology of the polishing pad, the distribution of abrasive particles, the chemical reaction between workpiece and polishing slurry, the polishing process parameters, the material properties of workpiece, and the parameters of ultrasonic vibration.

This paper is organized into six sections. Following Sect. 1, Sect. 2 describes the ultrasonic elliptical vibration-assisted chemical mechanical polishing experimental setup. In Sect. 3, the effects of ultrasonic vibration on chemical reaction occurred between reagent and workpiece, and mechanical impact wear of abrasive particles on workpiece surface is studied, respectively. In Sect. 4, a novel material removal model of UEV-CMP is developed step by step. Section 5 provides the material removal model verification by design of experiments. Conclusions are contained in Sect. 6.

2 Experimental setup of UEV-CMP

The ultrasonic elliptical vibration can be synthesized by two ultrasonic vibrations in orthogonal directions with the same frequency [20–21]. A schematic of the ultrasonic elliptical vibration transducer combined by a longitudinal vibrator and a bending vibrator is illustrated in Fig. 1. The transducer consists of one end cap, two ring-disk-shaped piezo-electric actuators, one middle cap, two pairs of half ring-disk-shaped actuators with anti-polarity, and one front cap, which are bonded together by a bolt. The exciting alternating current with high frequency generated by an ultrasonic generator is transported to the ring-disk-shaped piezoelectric ceramic transducer (PZT) actuators and the half ring-disk-shaped PZT actuators, which generate longitudinal vibration and bending vibration, respectively, under the converse piezoelectric effect. The direction of longitudinal vibration and the direction of bending vibration are orthogonal. The longitudinal ultrasonic vibration wave signals generated by the ring-disk-shaped actuators and the bending ultrasonic vibration wave signals generated by the half ring-disk-shaped actuators with anti-polarity can be transferred to the workpiece by the ultrasonic horn. When two alternating current voltages with a phase difference are applied to the PZT at the same frequency that is close to the resonant frequency of the longitudinal mode and bending mode of

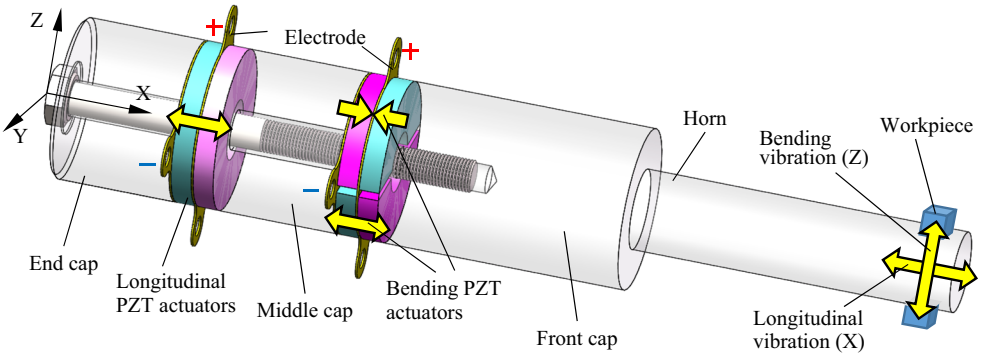

Fig. 1 A schematic of ultrasonic elliptical vibration device

vibrator, two ultrasonic vibrations are generated simultaneously, and synthesis of the two vibrations results in an elliptical motion on the end face of the vibrator. Therefore, the workpiece attached on an elliptical vibrator can also vibrate simultaneously in two directions with composite of longitudinal ultrasonic vibration and bending ultrasonic vibration. At the same time, the vibration amplitude of the workpiece fixed at the end of the horn is amplified by the horn. Then, high material removal rate and high surface quality in polishing are expected because two different vibrations are synthesized and rubbing directions of the polishing particles appear random at the micro-scale of the workpiece surface [20–21].

Ultrasonic elliptical vibration-assisted chemical mechanical polishing experiments are performed on a UEV-CMP machine designed by ourselves. The schematic of the UEV-CMP setup designed for the polishing experiments is illustrated in Fig. 2. The experimental setup mainly consists of an ultrasonic elliptical vibration device and a polishing machine. The polishing pressure can be adjusted by changing the weight on the node point of horn, because the node point does not vibrate at all; the loads applied to this point have no influence on the ultrasonic vibration amplitude of workpiece fixed at the end of the horn, which has been testified by ANSYS analysis. The polishing slurry can be provided to the interface between polishing pad and workpiece; then, the surface material of workpiece is removed by the combined actions of ultrasonic vibration and conventional CMP. This experimental setup is convenient to work as ultrasonic vibration-assisted CMP or conventional CMP governed by the operation of the two switches to control the ultrasonic generator. As shown in Fig. 2, when both the switch 1 and the switch 2 are turned off, the workpiece does not vibrate; this polishing process is called conventional CMP (C-CMP). When the switch 1 is turned on and the switch 2 is turned off, the workpiece just vibrates ultrasonically along horizontal direction; this polishing process is called ultrasonic horizontal vibration-assisted CMP (UHV-CMP). When the switch 1 is turned off and the switch 2 is turned on, the workpiece just vibrates ultrasonically along vertical direction; this polishing process is called ultrasonic vertical vibration-assisted CMP (UVV-CMP). When both the switch 1 and the switch 2 are turned on, the workpiece vibrates ultrasonically along an elliptical trajectory; this polishing process is called UEV-CMP. The ultrasonic generator converts 50-Hz electrical supply to high-frequency (20~50 kHz) AC output. Under the circumstances, the workpiece fixed at the end of horn also vibrates at the same frequency. In general, the vibration amplitude correlates roughly linearly to input voltages manifested by experiments [18]. When the output power of the ultrasonic generator is 180 W, the amplitudes of the workpiece are 3 and 2.5 μm in horizontal direction and vertical direction, respectively, measured by laser Doppler vibration meter (LK-G5001V by KEYENCE Corp.) equipped with respective sensors. The phase difference between the horizontal vibration and the vertical vibration keeps a constant of $\pi/2$, so the synthesis of the two vibrations yields nearly an elliptical vibration trajectory, as shown in Fig. 3.

3 Pilot experiments

3.1 Polishing performance confirmation of the experimental setup of UEV-CMP

A series of designed polishing experiments are conducted to evaluate the performances of the ultrasonic elliptical vibration-assisted chemical mechanical polishing machine developed by us. The experimental conditions of the pilot polishing experiments are listed in Table 1. The workpiece material used in the pilot experiments is monocrystalline silicon. The workpiece size is 10 × 10-mm area, and its initial surface roughness is about R_a 0.2 μm. The material employed in the pilot experiments is made up of abrasive particles of silica (SiO_2), and the abrasive size of silica particle is about 50 nm. Its polishing slurry contains 2% silica particles, and the pH value is about 9. Diethanolamine and ethylenediamine are used as pH value regulator and dispersant, respectively. The slurry feed rate is about 15 mL/min. The polishing pad is porous polyurethane pad, and its thickness is about 1.5 mm. The polishing experiments are divided into four different groups. Twenty workpieces are polished in each experiment of conventional CMP, UHV-CMP, UVV-CMP, and UEV-

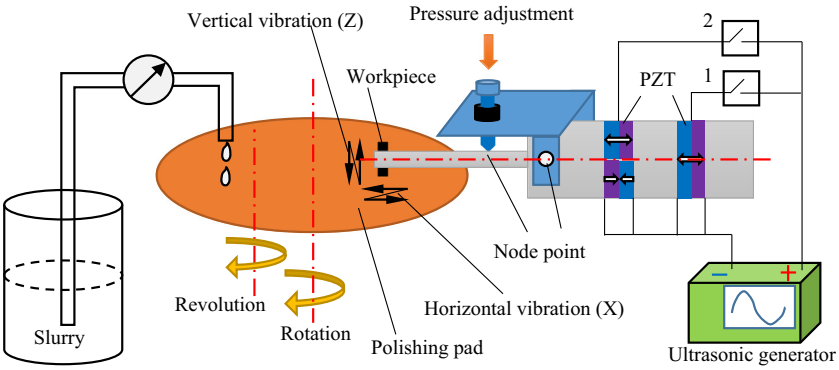

Fig. 2 Schematic of ultrasonic elliptical vibration-assisted CMP experimental setup

CMP by the operation of the two switches to control the output signals of the ultrasonic generator shown in Fig. 2. The silicon specimens are cleaned by ultrasonic vibration with acetone and dried by N_2-blown flow. The MRR is determined on the basis of weight loss of workpieces before and after polishing. The surface roughness values and morphologies of the polished silicon workpieces are measured and observed by Veeco profilometer equipment.

The MRRs of the workpieces polished by conventional CMP, UHV-CMP, UVV-CMP, and UEV-CMP are 320.1, 565.2, 469.7, and 693.6 nm/min, respectively, as shown in Fig. 4. It can be known that the material removal rate is indeed increased by introducing ultrasonic vibration into conventional CMP; especially, the MRR of UEV-CMP increases significantly compared to that of conventional CMP. In addition, the relation between surface roughness and polishing process is also plotted in Fig. 4. The average surface roughness R_a values of 20 workpieces polished by conventional CMP, UHV-CMP, UVV-CMP, and UEV-CMP are 27.61, 19.94, 16.14, and 10.61 nm, respectively. It can be seen from Fig. 4 that the surface roughness of the workpieces polished by conventional CMP, UHV-CMP, UVV-CMP, and UEV-CMP, respectively, decrease significantly. Hence, ultrasonic vibration has significant effect on the MRR and surface roughness of workpiece polished by CMP. Especially, both the MRR and surface quality are improved greatly when the workpieces are polished by UEV-CMP. The surface morphology of a workpiece polished by UEV-CMP is shown in Fig. 5. It can be seen from Fig. 5 that there is nearly no scratches and bulges on the surface polished by UEV-CMP. Therefore, it is obvious from the experiments that UEV-CMP is effective to improve the polishing quality and polishing efficiency to the greatest extent than

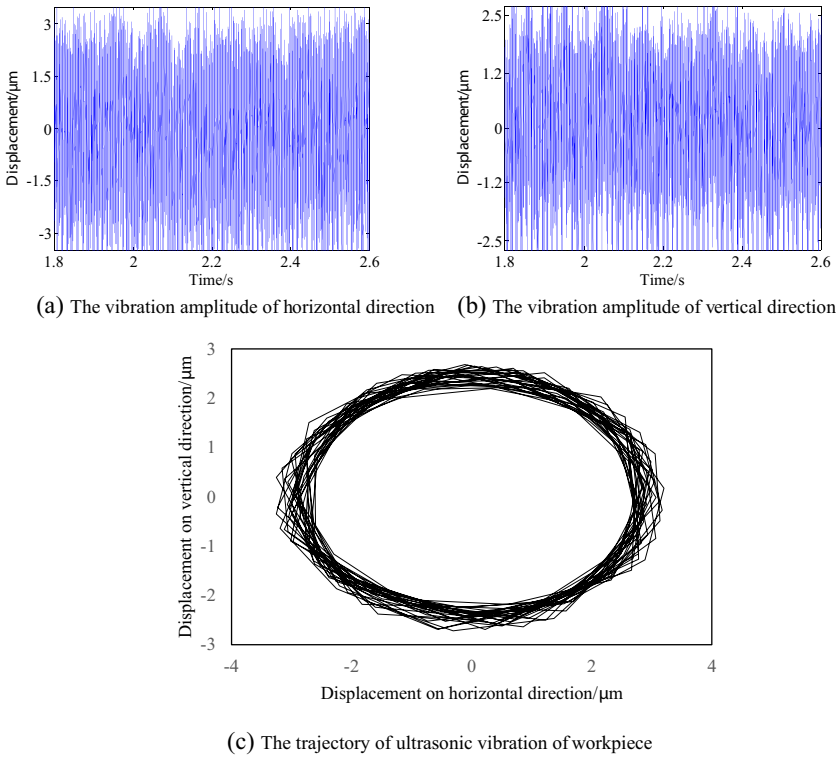

(a) The vibration amplitude of horizontal direction (b) The vibration amplitude of vertical direction

(c) The trajectory of ultrasonic vibration of workpiece

Fig. 3 The amplitude and trajectory of ultrasonic vibration of the workpiece. **a** The vibration amplitude of horizontal direction. **b** The vibration amplitude of vertical direction. **c** The trajectory of ultrasonic vibration of the workpiece

Table 1 Experimental conditions of CMP

Polishing variables	Value	Polishing variables	Value
Polishing time/min	30	Rotation speed of pad/(r min^{-1})	3
Abrasive size of particles/nm	50	Revolution speed of pad/(r min^{-1})	30
Slurry density/(g cm^{-3})	0.96	Polishing pressure/kPa	51.43
Concentration of abrasive particles	2%	Ultrasonic vibration frequency/kHz	35.3
pH value of slurry	9	Horizontal ultrasonic amplitude/μm	3
Slurry feed rate/(mL min^{-1})	15	Vertical ultrasonic amplitude/μm	2.5

other kinds of polishing methods. It indicates that the combined actions of ultrasonic elliptical vibration and conventional CMP can facilitate better polished surface and higher MRR. So, it is essential to investigate the effects of ultrasonic vibration on chemical reaction of polishing solution and mechanical impact of abrasive particles during UEV-CMP in order to explain how UEV-CMP improves MRR and quality compared to the conventional CMP.

3.2 The effects of ultrasonic vibration on chemical reaction between reagent and workpiece

To clearly analyze the roles of the ultrasonic elliptical vibration in chemical mechanical polishing process, the effects of ultrasonic vibration on chemical reaction of polishing solution and mechanical wear of abrasive particles are studied in Sects. 3.2 and 3.3, respectively, by design of experiments.

Hard and brittle materials such as monocrystalline silicon have very high chemical stability in natural environment. However, in alkaline or acidic polishing solution, it plays a very important role in revealing the material mechanism to investigate whether chemical reaction is occurring in the material surface or not. Experiments of ultrasonic vibration-assisted chemical reaction are conducted to evaluate the effects of ultrasonic vibration on chemical reaction occurring between polishing solution and monocrystalline silicon specimens. The size of the specimens used in the chemical reaction experiments is same with that of the workpiece used in the above UEV-CMP experiments. The original specimens are cleaned by ultrasonic vibration in absolute ethyl alcohol and deionized water, respectively. The chemical reagent used in the experiment is NaOH alkaline solution with concentration of 2 mol/L. The specimens are fixed at the end of the horn of the ultrasonic elliptical vibration device as shown in Fig. 1, and they are immersed in the NaOH solution. The experiments are performed for 30 min of ultrasonic elliptical vibration, respectively, to compare the effects. The frequency of the ultrasonic elliptical vibration is 35.3 kHz. Figure 6 shows the experimental process of chemical reaction that occurred between reagent and silicon specimen with or without assistant of ultrasonic vibration.

The surface morphologies of the original specimen, the specimen corroded by NaOH solution without assistance of ultrasonic vibration, and the specimen corroded by NaOH solution with assistance of ultrasonic vibration are shown in Fig. 7. The roughness value of the original surface is only 8.62 nm. There is nearly no pits on the surface of specimen. However, the roughness value of the specimen surface corroded by NaOH solution without assistant of ultrasonic vibration is 20.28 nm with obvious sags and crests, while the roughness value of the specimen surface corroded by NaOH solution with assistant of ultrasonic elliptical vibration increases to 191.66 nm with extreme wrinkles, which indicates that violent chemical reaction has occurred. The results indicate that the ultrasonic elliptical vibration can increase the speed of chemical reaction significantly. Therefore, the material removal during UEV-CMP process could be depicted as the continuous formation and removal of the soft layer with relative lower hardness than silicon.

During the process of ultrasonic vibration-assisted chemical reaction that occurred between polishing solution and specimen, the energy (E_u) imposed on the unit amount substance of the chemical erosion layer on the specimen surface by ultrasonic vibration can be expressed by the following equation:

$$E_u = \frac{W}{n} = \frac{mv^2}{2n} = \frac{\rho S \Delta h \omega^2 A^2 \sin^2(\omega t - \varphi)}{2000 \rho S \Delta h \Big/ M} = 2 \times 10^{-3} M \omega^2 A^2 \sin^2(\omega t - \varphi) \quad (1)$$

where

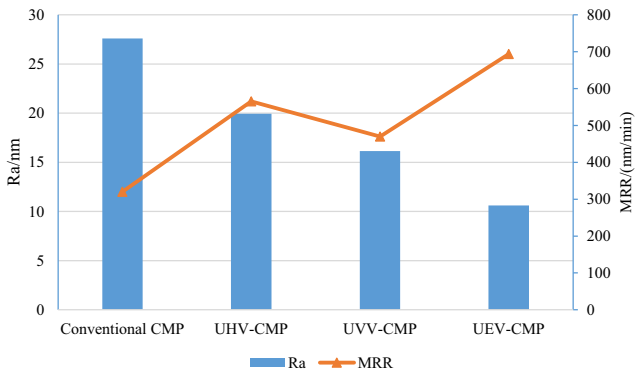

Fig. 4 The relations between MRR, roughness, and polishing process

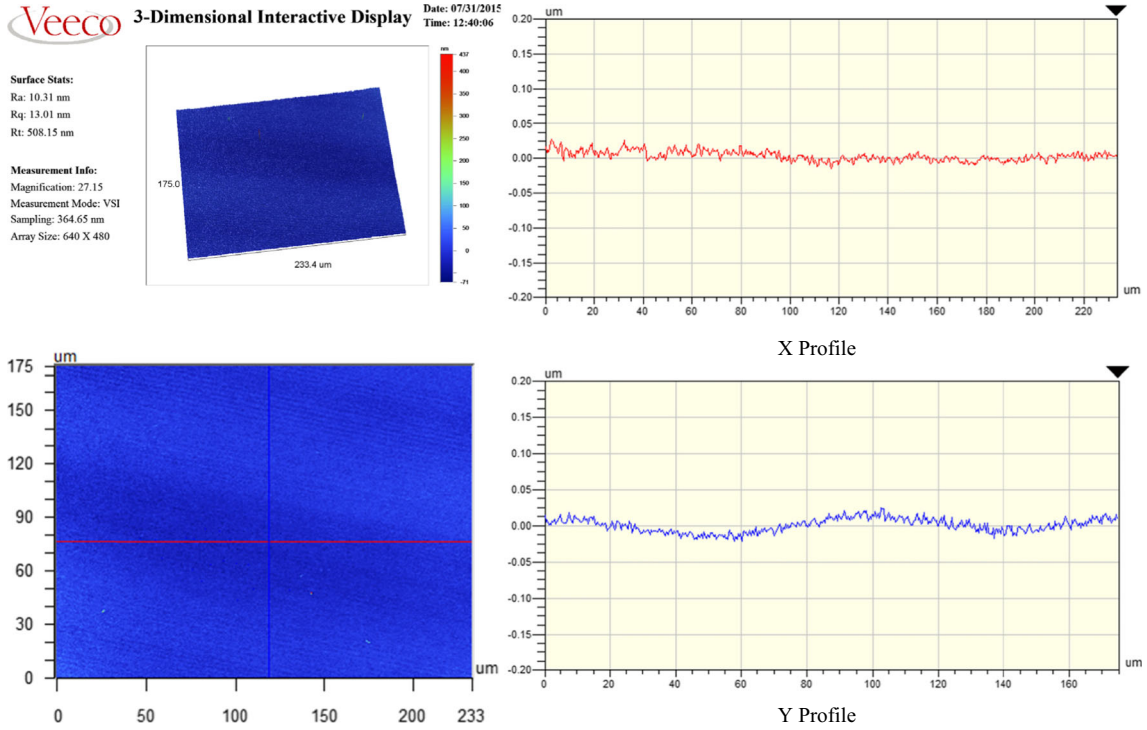

Fig. 5 Morphology of a monocrystalline silicon polished by UEV-CMP

W is the kinetic energy of ultrasonic vibration of the workpiece (J);
n is the amount of substance of the reaction layer (mol);
S is the area of surface corroded under assistant of ultrasonic vibration (m^2);
ρ is the density of specimen (kg/m^3);
ω is the angular frequency of ultrasonic vibration, $\omega = 2\rho f$ (rad/s);
A is the amplitude of ultrasonic vibration (m);
Δh is the thickness of the chemical reaction layer; and
M is the molar mass of reactants (g/mol).

According to the theory of chemical reaction thermodynamics and ultrasonic chemistry, the energy of the surface atoms of the polished specimen increased by ultrasonic vibration and additives can improve the chemical reaction speed. Therefore, the chemical reaction rate k_c can be expressed by the following Arrhenius-type relation [23]:

$$k_c = k_0 e^{-\frac{E_a - E_u - E_s}{RT}} \tag{2}$$

where

k_0 is a frequency factor;
E_a is the original activation energy (J/mol);
E_s is the activation energy by oxidant, erosion inhibitor, chelating agent, and other additives, (J/mol);
R is the Boltzmann constant, R = 8.314 J/(mol K); and
T is the absolute temperature (K).

It can be seen from Eq. (2) that the chemical reaction rate k_c increases with ultrasonic vibration energy E_u.

3.3 The effects of ultrasonic vibration on mechanical abrasive wear of particles

In chemical mechanical polishing, the abrasive particles are mixed with the polishing solution to be supplied to the process. Since the abrasive particles are suspended in the fluid, in principal, they are able to roll freely between workpiece and the polishing pad or to penetrate into the asperities of the polishing pad losing the freedom of rotation. The abrasive particle motion between the workpiece surface and the polishing pad determines the main wear mechanism, whereas the different wear mechanisms lead to different distinct surface morphologies. The wear mechanism of the workpiece during UEV-CMP should be classified as abrasive wears.

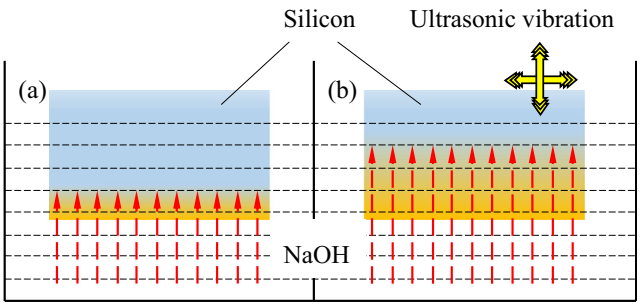

Fig. 6 Chemical reaction experiments **a** without assistant of ultrasonic vibration and **b** with assistant of ultrasonic vibration

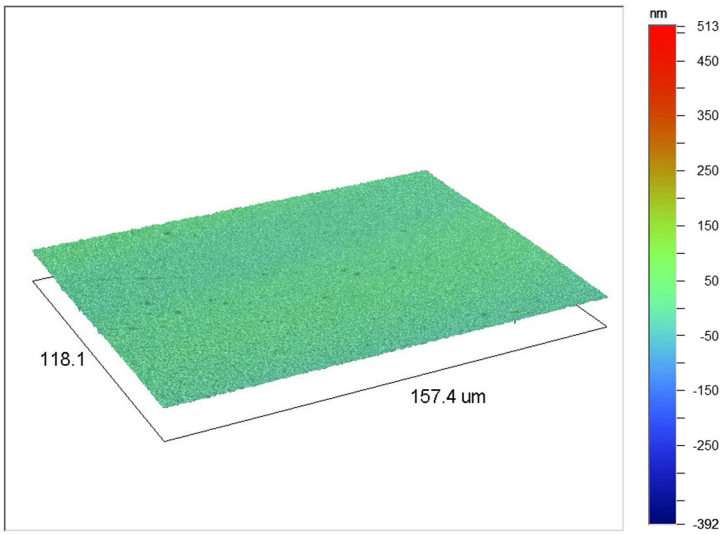

(a) R_a=8.62nm

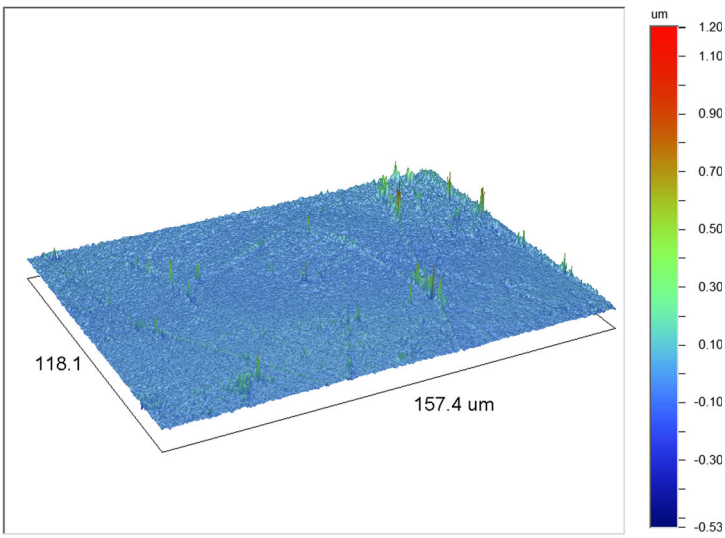

(b) R_a=20.28nm

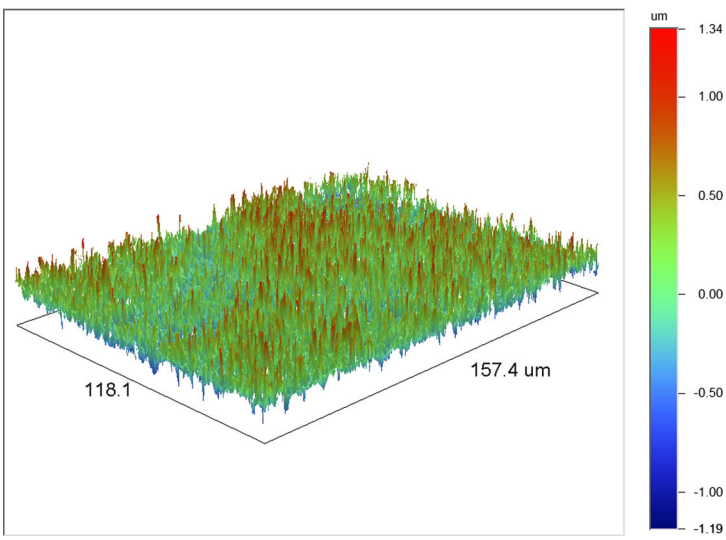

(c) R_a=191.66nm

Fig. 7 **a** The original surface of specimen, **b** the surface corroded by NaOH solution without assistant of ultrasonic vibration, and **c** the surface corroded by NaOH solution with assistant of ultrasonic elliptical vibration

Abrasive wear includes the two-body abrasive wear and three-body abrasive wear. The two-body abrasive wear refers to the micro-cutting or micro-plowing produced by the embedded abrasive particles between interaction surfaces, while the three-body abrasive wear refers to the micro-indentation or micro-cracking caused by the free rolling abrasive particles in the contact zone. The wear coefficient decreases when the ultrasonic vibration is introduced, which contributes to the transition from two-body abrasion to three-body abrasion [17]. Therefore, only a few abrasive particles fixed in the asperities of the polishing pad emerge micro-plowing behavior, while most of other abrasive particles rolling between the polishing pad and workpiece surface exhibit micro-indentation behavior. Thus, the three-body abrasive wear can be formed among the workpiece, the polishing pad, and the abrasive particles. In this case, the low impact will lead the abrasive particles to produce only rolling extrusion or squeezing on the workpiece surface instead of micro-plowing or micro-cutting. The two-body abrasive wear mechanism can be converted to the three-body abrasive wear mechanism when the ultrasonic vibration is introduced into the conventional CMP process. Moreover, with the increasing of amplitude and frequency of the ultrasonic vibration, the three-body abrasive wear will take a bigger proportion over two-body abrasive wear [17].

Therefore, while the ultrasonic vibration energy is transmitted to the numerous abrasive particles in the polishing slurry, the suspended particles may impact on the workpiece surface in an isotropic manner, and the material of the workpiece surface is removed by these numerous repetitive three-body abrasive wear caused by impact at very high frequency. For the purpose of confirming the mechanical abrasive wear of particles to the workpiece surface during UEV-CMP, the experiments of impact wear of abrasive particles on specimen are designed. The material of specimens is monocrystalline silicon, and the size of the specimen is also 10 × 10-mm length. The specimens are put into the deionized water polishing slurry with SiO_2 nanoparticles for 30 min, as shown in Fig. 8. Ultrasonic vibration is imposed on the specimen through the ultrasonic vibration device shown in Fig. 1. The frequency of the ultrasonic vibration is also 35.3 kHz.

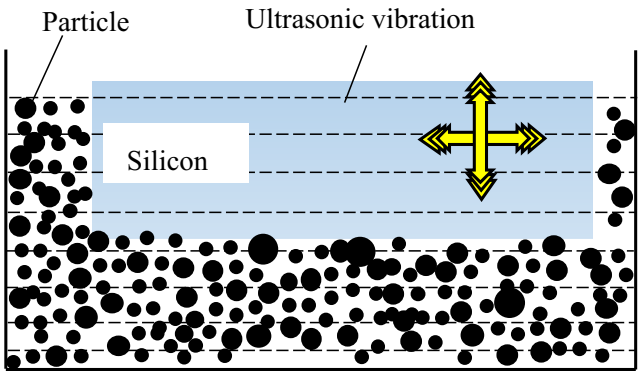

Fig. 8 The effects of ultrasonic vibration on mechanical impact wear of abrasive particles

The surface morphology of a specimen impacted by SiO_2 particles in deionized water with assistant of ultrasonic vibration is shown in Fig. 9. The experimental results indicate that the SiO_2 particles cause obvious pits on the specimen surface, which meets well with the impact abrasive wear theory [24]. Therefore, the three-body abrasive wear mechanism (micro-indentation) exists in the UEV-CMP process besides the two-body abrasive wear mechanism (micro-plowing).

4 Development of material removal rate model

It can be seen from above pilot experiments that a soft layer on workpiece surface formed by the chemical action of the polishing slurry is removed not only by the mechanical action of conventional CMP but also by the ultrasonic vibration of UEV-CMP. The MRR increases significantly when the UEV-CMP is used to polishing monocrystalline silicon workpieces due to the combined actions of ultrasonic vibration and conventional CMP. The UEV-CMP is a complex process with a large number of input variables, as shown in Fig. 10. In order to describe the effects of ultrasonic elliptical vibration on MRR, a novel material removal rate model of UEV-CMP is developed. To develop the model, the following approaches are carried out step by step:

(1) Develop a morphology model to depict the characteristics of the polishing pad surface;
(2) Obtain the number of the abrasive particles actually taking part in polishing;
(3) Estimate V_i, the actual material volume removed by one particle in a single ultrasonic vibration cycle in horizontal direction and vertical direction respectively, which combine an ultrasonic elliptical vibration;

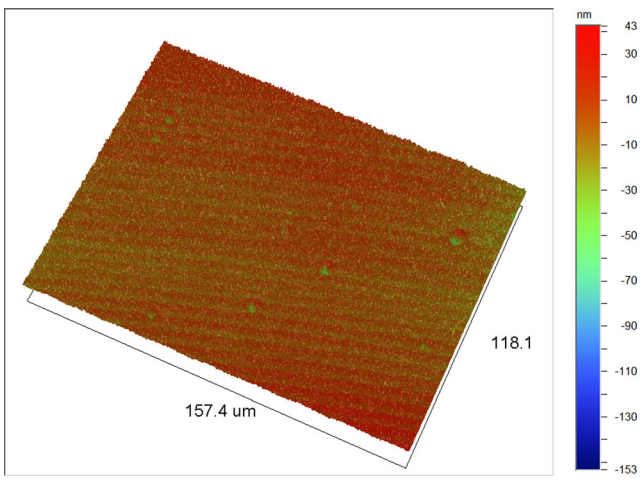

Fig. 9 Surface morphology of specimen impacted by SiO_2 particles in deionized water with assistant of ultrasonic vibration, R_a = 12.68 nm, ×40

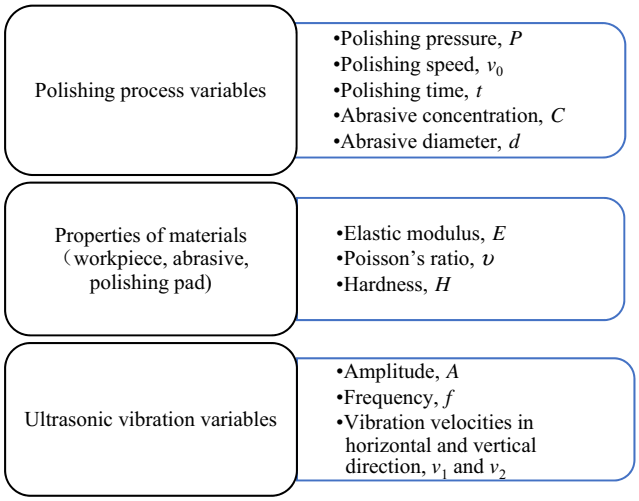

Fig. 10 Input variables in development of material removal rate model for UEV-CMP

(4) Develop the material removal model under horizontal and vertical direction vibration by aggregating the effects of all active abrasive particles;
(5) Establish the overall material removal model of UEV-CMP based on the material removal models of the ultrasonic elliptical vibration.

The contact among workpiece, polishing pad, and abrasive particles during the UEV-CMP process is illustrated in Fig. 11. The workpiece can vibrate ultrasonically with the velocity of v_1 and v_2 in horizontal and vertical directions, respectively. At the same time, the polishing pad is driven by the polishing machine at the centrifugal rotary velocity of v_0. In addition, there is an assumption that the abrasive particles distribute uniformly in the polishing slurry.

4.1 Contact between polishing pad and workpiece

The micro-morphology of a polishing pad should be described accurately to evaluate the mechanism of CMP. The mainly models reported for describing the morphology of a polishing pad include hemisphere model with equal radius [25], rough peak model of equal radius of curvature [25], and hemisphere contact model [26], which can partly explain the contact in CMP process. However, it is hard for them simultaneously to explain the effect of polishing pressure on the real contact area between pad and workpiece and to depict properly the contact between a single particle and workpiece. The material of the polishing pad used in this paper is polyurethane. The morphologies of the polishing pad observed by SEM and laser scanning confocal microscope are shown in Figs. 12 and 13, respectively. It can be seen from the two figures that the height and the span of the micro-concave and convex bodies are not equal. It is unreasonable to simplify the concave to sphere. Therefore, a more reasonable model is proposed to describe the morphology of the polishing pad surface, in which the height of the sine-shaped micro-concave and convex bodies obey normal distribution and the diameters of them obey γ distribution.

The size distribution of projection circle of concave and convex bodies of the polishing pad is shown in Fig. 14. It can be seen from the Fig. 14 that the diameter distribution is not normal distribution but approximately γ distribution.

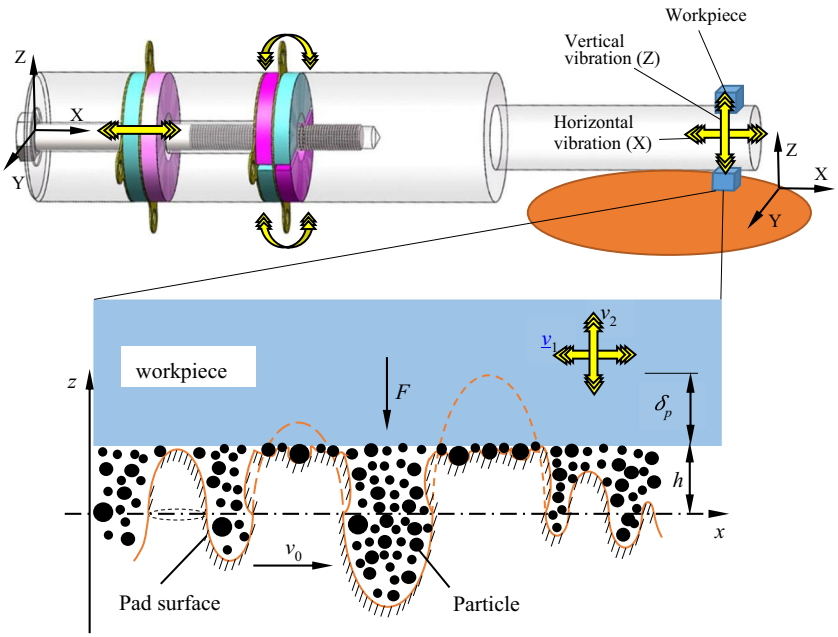

Fig. 11 The contact among workpiece, polishing pad, and abrasive particles

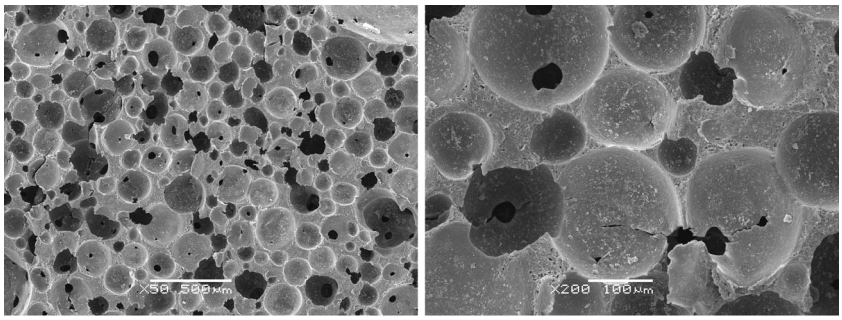

Fig. 12 Surface morphology of the polishing pad observed by SEM

Therefore, the diameter distribution $\varphi(d_p)$ of projection circle of concave and convex bodies on average plane of contact region can be described by the following equation:

$$\varphi(d_p) = \frac{\lambda^{\gamma} d_p^{\gamma-1}}{\Gamma(\gamma)} e^{-\gamma d_p} \tag{3}$$

Based on probability statistical theory, the overall distribution can be estimated according to the distribution of a polishing pad sample selected randomly. Then, parameter estimation can be performed based on the data of the sample and γ distribution function; therefore, the diameter distribution $\varphi(d_p)$ can be obtained by the following equation:

$$\varphi(d_p) = \frac{0.0275^{2.8} d_p^{1.8}}{\Gamma(2.8)} e^{-2.8} d_p \tag{4}$$

Sample Kolmogorov-Smirnov test is a stable and widely applicable method of hypothesis tests. The hypothesis test results of the above parameter estimation are listed in Table 2, which are obtained by MATLAB software.

It is known from the hypothesis test results in the Table 2 that the parameter estimation expressed by Eq. (4) is very reasonable. The integral distribution curves of the estimating result and the sample are shown in Fig. 14b. According to the γdistribution, the average diameter $E(d_p)$ of projection circle can be described by the following equation:

$$E(d_p) = \frac{\lambda}{\gamma} \tag{5}$$

The roughness of the polishing pad surface is generally at micrometer scale, while the roughness of the workpiece surface is at nanometer scale. Therefore, the contact between polishing pad and workpiece can be equivalent to a kind of contact between a rough surface and an ideal smooth surface. To simplify the contact between the polishing pad and workpiece, there are two hypotheses for the polishing pad listed as the following:

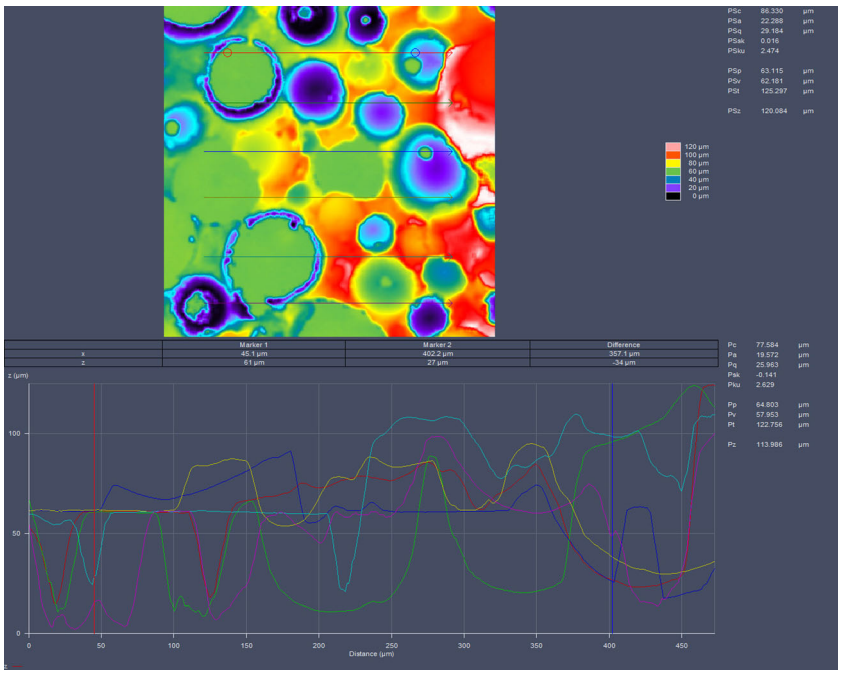

Fig. 13 The cross section of the polishing pad observed by laser scanning confocal microscope

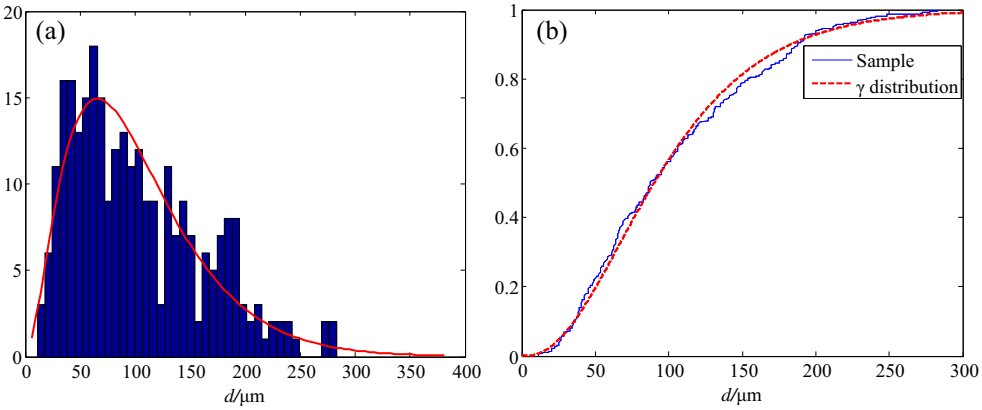

Fig. 14 **a** Histogram and **b** integral distribution curves of projection circle of concave and convex bodies

1. The polishing pad surface contains micro-concave and convex bodies with the sine shape in *xoz* plane, as shown in Fig. 15;
2. The height of the sine-shaped micro-concave and convex bodies obeys normal distribution.

The height of single sine-shaped body $z_i(x)$ can be described by the following equation:

$$z_i(x) = z_{\text{im}} \sin\left(\frac{\pi}{D_i}x + L_{i-1}\right), \quad x \in (0, \ D_i) \tag{6}$$

where

z_{im} is the height of a convex body when $z_{\text{im}} > 0$ or the pit when $z_{\text{im}} < 0$,
L_{i-1} is the distance between a convex body i and origin point, and
D_i is the diameter of the projection circle of a convex body on average plane.

The radius of the contact area is the radius of curvature R_{pi}, which is given by the following equation:

$$R_{\text{pi}} = \left.\frac{\left[1 + z_i'^2(x)\right]^{3/2}}{|z_i''^2(x)|}\right|_{x \ = \ 0.5d_i} = \frac{D_i^2}{\pi^2 |z_{\text{im}}|} \tag{7}$$

The height of the sine-shaped micro-concave and convex bodies obeys vertical distribution $N(m,\sigma)$,

$$p(z_{\text{im}}) = \frac{1}{\sigma\sqrt{2\pi}} \exp\left[-\frac{(z_{\text{im}} - m)^2}{2\sigma^2}\right] \tag{8}$$

where

p is the frequency function of height amplitude of micro-body of the pad,
m is the average plane which is 0 plane in this model, and
σ is the standard deviation of height amplitude.

If there is an assumption that the number of convex bodies is equal to the number of pit, σ can be expressed for Gauss surface as [18]

$$\sigma \approx \sqrt{\frac{\pi}{2}} R_a \tag{9}$$

Therefore, the vertical distribution $N(m,\sigma)$ can be obtained from surface roughness R_a.

The pressure produced by the polishing fluid flow on the polishing pad can be neglected because it is relatively small during CMP; therefore, the contact rough peaks of the polishing pad support all the working pressure [27]. When the bottom surface of workpiece reaches to the position where h is far away from the average plane under polishing static pressure, it contacts with the micro-convex body whose height is larger than h as shown in Fig. 15. Then, the possibility P_c for micro-convex body to contact with workpiece can be calculated by the following equation:

$$P_c(z > h) = \int_h^{\infty} p(z)dz \tag{10}$$

The number of contacted micro-convex body can be calculated by the following equation:

Table 2 Kolmogorov-Smirnov test results

Variable	Description	Explanation	Test result
h	Hypothesis test result	0 Accept the original hypothesis 1 Refuse the original hypothesis	0
p	The probability of the occurrence of the null hypothesis	Accept the original hypothesis when $p > 0.05$	0.5721
α	Significance level of the hypothesis test		0.05
k_s	Test statistic of the hypothesis test	Accept the original hypothesis when	0.0461
c_v	Critical value	$c_v > k_s$	0.0804

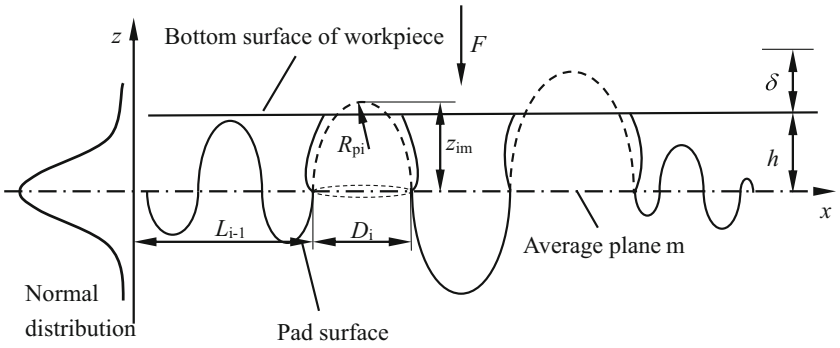

Fig. 15 The simplified model of the polishing pad

$$n_c = N\int_h^{\infty} p(z)dz = \frac{4A_0}{\pi E^2(d_p)}\int_h^{\infty} p(z)dz \tag{11}$$

where

N is the total number of micro-convex bodies,
A_0 is the area of bottom surface of workpiece, and
$E(d_p)$ is the average diameter of projection circle of concave and convex bodies on average plane.

Owing to $\delta = z - h$, the real contacted area A_{re} can be described by the following equation:

$$A_{re} = \pi N\int_h^{\infty}\int_0^{+\infty} R_p(z-h)p(z)p(R_p)dz\ dR_p \tag{12}$$

Therefore, the total load F supported by the polishing pad can be described by the following equation:

$$F = \frac{4}{3}NE_{pw}\int_h^{+\infty}\int_0^{+\infty} R_p^{\frac{1}{2}}(z-h)^{\frac{3}{2}}p(z)p(R_p)dz\ dR_p \tag{13}$$

where $E_{pw} = \left(\frac{1-v_p^2}{E_p} + \frac{1-v_w^2}{E_w}\right)^{-1}$ is the equivalent Young's modulus of the polishing pad and workpiece; E_p and E_w are the Young's modulus of the polishing pad and workpiece, respectively; and 劉$_p$ and劉$_w$ are the Poisson's ratio of the polishing pad and workpiece, respectively.

Therefore, the pressure imposed on by the polishing pad can be calculated by the following equation:

$$P = \frac{F}{A_0} = \frac{4}{3A_0}NE_{pw}\int_h^{+\infty}\int_0^{+\infty} R_p^{\frac{1}{2}}(z-h)^{\frac{3}{2}}p(z)p(R_p)dz\ dR_p \tag{14}$$

The polishing pad deformation δ_{asp} can be determined by the following equation:

$$\delta_{asp} = h_0 - h \tag{15}$$

where h_0 is the height of the highest peak of the polishing pad, which is approximately 3σ.

The relationship between polishing pressure P and the relative position of bottom surface of the workpiece and polishing pad deformation δ_{asp} can be obtained based on Eq. (14) according to the parameters listed in Table 3, as shown in Fig. 16. When the polishing pressure is 50 kPa and the roughness of pad is 6 μm, it is observed from Fig. 16 that the position of workpiece relative to the polishing pad is 5.95 μm and the pad deformation δ_{asp} is 16.61 μm.

4.2 Number of active particles taking part in polishing

The material of workpiece is removed by the abrasive particles in the contact region of pad/particle/workpiece. The number of particles actually taking part in polishing and grain size of the particles are the two key factors that affect the material removal rate in CMP [28].

The number of total particles N_r in the contact region between workpiece and polishing pad can be obtained by the following equation proposed by Jeng [29]:

$$N_r = \frac{6A_0(3\sigma - h)\rho_s c}{\pi\rho_a \overline{D}^3} \tag{16}$$

where

A_0 is the nominal contact area (area of bottom surface of workpiece),
ρ_s is the density of the polishing slurry,
c is the quality concentration of abrasive particles,
ρ_a is the density of particle, and
$\overline{D}$ is the average grain size of particles.

The number N_a of particles in three-body contact region can be determined by the following equation:

Table 3 Material properties of the polishing pad and workpiece

Variable	Description	Value	Unit
A_0	Area of bottom surface of workpiece	6.25	mm^2
E_p	Young's modulus of pad	0.01	GPa
v_p	Poisson ratio of pad	0.5	–
R_a	Roughness of pad	6	μm
$E(d_p)$	The average diameter of projection circle	36.35	μm
E_w	Young's modulus of workpiece	190	GPa
v_w	Poisson ratio of workpiece	0.28	–
E^*	Effective Young's modulus	1.33×10^7	Pa

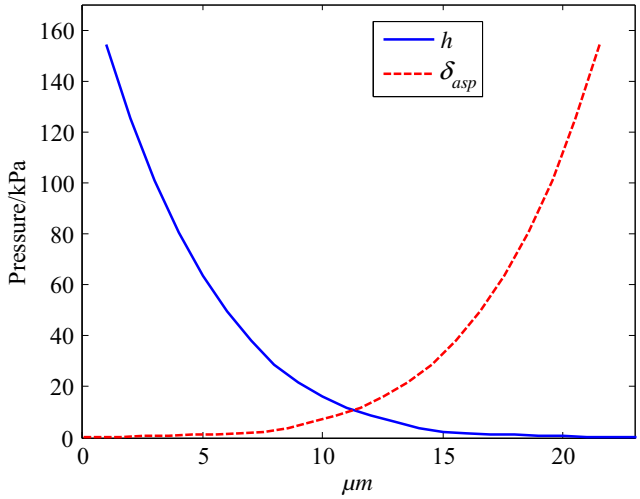

Fig. 16 The relationship between polishing pressure P and **a** the workpiece position h and **b** polishing pad deformation δ_{asp}

$$N_a = n_r A_{re} = \frac{N_r}{A_0} A_{re} = \frac{6(3\sigma - h)\rho_s c}{\pi \rho_a \overline{D}^3} A_{re} \tag{17}$$

where

n_r is the number of particles in unit area and
A_{re} is the real contact area.

4.3 Material removal rate model of UEV-CMP

When the ultrasonic vibration is introduced in the conventional chemical mechanical polishing, the material is removed by the complicated combined effects of the chemical reaction, the two-body micro-plowing, and three-body micro-indentation assisted by ultrasonic vibration. Ultrasonic elliptical vibration is synthesized by horizontal vibration and vertical vibration with the same frequency, which is described in Sect. 2. Therefore, several major reasonable assumptions and simplifications are made for the material removal model, which are as follows:

(1) The material removed by UEV-CMP can be treated as the combined effects of UHV-CMP and UVV-CMP.
(2) The material of workpiece is removed by micro-plowing of the particles assisted by the chemical reaction during the conventional CMP and the UHV-CMP.
(3) The material of workpiece is removed by micro-indentation of abrasive particles assisted by the chemical reaction during UVV-CMP.
(4) The material of workpiece is removed by both micro-plowing and micro-indentation with the assistance of chemical reaction during UEV-CMP.

4.3.1 The material removal rate model of particle's micro-plowing under ultrasonic horizontal vibration

When the workpiece vibrates ultrasonically in horizontal direction, the schematic of micro-plowing on workpiece surface caused by the spherical particles in contact region is illustrated in Fig. 17. Under this circumstance, the relative velocity u between workpiece and particle, which is synthesized by slurry flow velocity v_0 and ultrasonic vibration velocity v_1, is described by the following equation:

$$u = v_0 + v_1 = v_0 - 2A_H \pi f \cos(2\pi ft - \varphi) \tag{18}$$

where

A_H is the ultrasonic vibration amplitude in horizontal direction and
f is the ultrasonic vibration frequency.

When a particle scratches on workpiece surface, the scratch depth and width are 剜wi and $2a_i$, respectively, as shown in Fig. 17. The contact load between a single particle and workpiece F_{swi} can be determined by the following equation [30]:

$$F_{swi} = \frac{1}{2}\pi a_i^2 H_w \tag{19}$$

where H_w is the hardness of the workpiece.

The contact load between a single particle and polishing pad F_{spi} can be described by the following equation [26]:

$$F_{spi} = \frac{4}{3} E_{sp} R_{si}^{1/2} \delta_{pi}^{3/2} \tag{20}$$

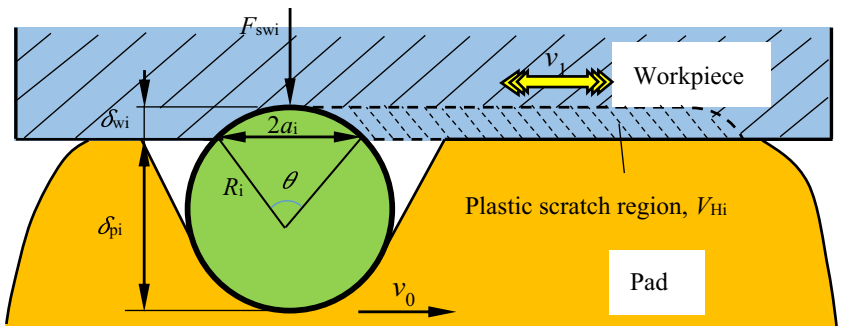

Fig. 17 Micro-plowing model of particles under ultrasonic horizontal vibration

where

$E_{sp} = \left(\frac{1-\nu_s^2}{E_s} + \frac{1-\nu_p^2}{E_p}\right)^{-1}$ is the equivalent Young's elastic modulus of the pad and particle,

E_s is the Young's modulus of the particle,

E_p is the Young's modulus of the pad,

ν_s is the Poisson's ratio of the particle, and

ν_p is the Poisson's ratio of the particle.

The material volume V_{Hi} removed by a single particle can be calculated by the following equation:

$$V_{Hi} = 2k_s k_c a_i \delta_{wi} x \tag{21}$$

Therefore, the total volume V_H removed by all of the particles actually taking part in polishing can be calculated by integrating Eq. (21) as

$$V_H = \int_0^{+\infty} 2k_s k_c a \delta_w x N_a p(R) dR \tag{22}$$

Then, the material removal rate MRR_H in the X direction of workpiece under ultrasonic horizontal vibration can be determined by

$$MRR_H = \frac{dV_H}{A_0 dt} = \frac{1}{A_0}\int_0^{+\infty} 2k_s k_c a \delta_w u N_a p(R) dR \tag{23}$$

where k_s is the wear coefficient of the particle and k_c is the frequency factor under chemical effects.

4.3.2 The material removal rate model of particle's micro-indentation under ultrasonic vertical vibration

When the workpiece vibrates ultrasonically in vertical direction, the micro-indentation model formed on the workpiece surface caused by particles is illustrated in Fig. 18. Based on Hutchings' theory, it can be assumed that the mass and shape of the particles in polishing slurry remain unchanged. From the contact moment ($t = 0$), the particle with the mass of m_i and the initial speed of v crashes into the workpiece surface to the depth of z ($t = t_0$). The cross section area of impact pit is $S(z)$. Therefore, the movement function of a single particle is determined by the following equation:

$$-HS(z) = m_i \frac{d^2 z}{dt^2} \tag{24}$$

The particle stops after moving for t_0 to a depth of d; then,

$$\int_0^d HS(z) dz = \frac{1}{2} m_i v_2^2 \tag{25}$$

The material volume V_{Vi} removed by the indentation pit of abrasive particle into silicon surface can be calculated by the following equation:

$$V_{Vi} = k_s \frac{m_i v_2^2}{2H} = k_s k_c \frac{2\pi \rho_a R_i^3 v_2^2}{3H} \tag{26}$$

Therefore, the total indentation volume V_V removed by all of the particles taking actually part in polishing can be calculated by the following equation:

$$V_V = \int_0^{+\infty} k_s k_c \frac{2\pi \rho_a R^3 v_2^2}{3H} N_r p(R) dR \tag{27}$$

Then, the material removal rate V_{VT} of a unit period of vertical ultrasonic vibration can be obtained by the following equation:

$$V_{VT} = \frac{1}{T}\int_0^T V_V dt = \int_0^{+\infty} k_s k_c \frac{2\pi \rho_a R^3 A_V^2 \omega^2}{3H} N_r p(R) dR \tag{28}$$

where A_V is the ultrasonic vibration amplitude in vertical direction.

Then, the material removal rate MRR_V in the Z direction of workpiece under ultrasonic vertical vibration can be described as follows:

$$MRR_V = \frac{V_{VT}}{A_0} = \frac{1}{A_0}\int_0^{+\infty} k_s k_c \frac{2\pi \rho_a R^3 A_V^2 \omega^2}{3H} N_r p(R) dR \tag{29}$$

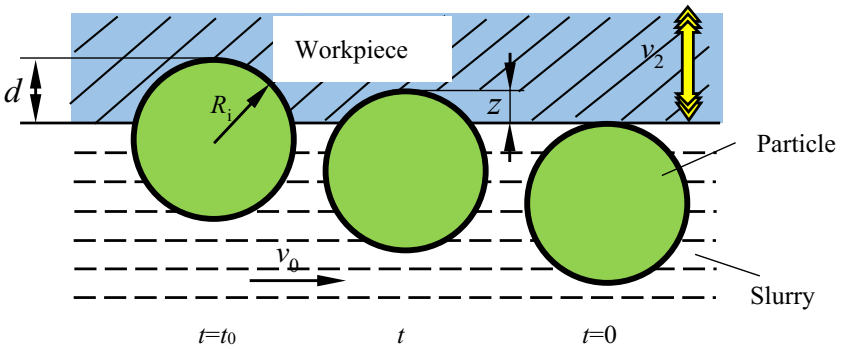

Fig. 18 Micro-indentation model of particles under ultrasonic vertical vibration

Table 4 Common experimental parameters of polishing variables for model verification

Polishing variables	Value	Polishing variables	Value
Slurry density/(/g cm^{-3})	0.96	Polishing slurry feed rate/(mL/min)	15
Abrasive size of particles/nm	50	Rotation speed of pad/(r/min)	3
pH value of slurry	9	Revolution speed of pad/(r/min)	30
Concentration of abrasive particles	2%	Polishing time/min	30

4.3.3 Material removal rate model synthesized by MRR_H and MRR_V

As the ultrasonic elliptical vibration is decomposed into a horizontal vibration component and a vertical vibration component with the same frequency, therefore, the total material removal rate of the UEV-CMP can be synthesized by Eq. (23) MRR_H and Eq. (24) MRR_V according to the achievement of elliptical trajectory,

$$\mathrm{MRR} = k\sqrt{\mathrm{MRR}_H^2 + \mathrm{MRR}_V^2} = \frac{kk_sk_c}{A_0}\sqrt{\left(\int_0^{+\infty} 2a\delta_w u N_a p(R)dR\right)^2 + \left(\int_0^{+\infty} \frac{2\pi\rho_a R^3 A_V^2\omega^2}{3H} N_r p(R)dR\right)} \quad (30)$$

Equation (30) represents the material removal rate model of UEV-CMP, and it should be pointed that the equation can also be used to compute the material removal rate of conventional CMP, UHV-CMP, or UVV-CMP through controlling input variables of ultrasonic vibration. Furthermore, it is obvious that Eq. (30) together with Eqs. (1), (14), (17), (23), and (29) could expound the roles played by the polishing variables in the UEV-CMP such as polishing pressure, vibration amplitude, and vibration frequency.

5 Experimental verification of theoretical model

To verify this MRR model, a series of experiments are conducted to compare the predicted and experimentally determined trends regarding effects of input variables (polishing pressure, ultrasonic vibration amplitude, and ultrasonic vibration frequency) on MRR.

5.1 Design of experiments

The theoretical model for material removal rate developed in above section is verified through a series of simulations and chemical mechanical polishing experiments. A simulation program is purposely developed by the authors for the implementation of the model using the MATLAB software package. In order to confirm the viability of the developed model, three sets of experiments are performed to verify the roles of polishing pressure, vibration amplitude, and vibration frequency.

The common experimental parameters of the polishing variables are listed in Table 4; these variables are held constant during all test runs. The workpiece material used in the polishing experiments is monocrystalline silicon. The workpiece size is 10 × 10-mm length, and its initial surface roughness is about R_a 0.2 μm. The material of the abrasive particles employed in the pilot experiments is silica (SiO_2), and the size of abrasive silica particles is about 50 nm. The polishing slurry contains 2% silica particles, and the pH value is about 9. The diethanolamine and ethylenediamine are used as pH value regulator and dispersant, respectively. The slurry feed rate is about 15 mL/min. The polishing pad is porous polyurethane pad, and its thickness is about 1.5 mm. The silicon specimens are cleaned by ultrasonic vibration in the acetone and dried by N_2-blown flow. The MRR is determined on the basis of weight loss of workpieces before and after polishing.

In order to verify the relation between MRR and polishing pressure, the experimental design undertaken is shown in Table 5. The polishing experiments involve four groups of input variables according to ultrasonic vibration type, including conventional CMP, UVV-CMP, UHV-CMP, and UEV-CMP. The polishing pressure varies from 22.85 to 80.01 kPa in each group.

In order to verify the relation between MRR and ultrasonic vibration, the experimental design followed is listed in

Table 5 Experimental conditions for model verification (MRR versus polishing pressure)

Experiment	Polishing type	Polishing pressure/kPa	Horizontal ultrasonic amplitude/μm	Vertical ultrasonic amplitude/μm	Ultrasonic vibration frequency/kHz
First group	C-CMP	22.85, 37.14, 51.43, 65.72, 80.01			35.3
Second group	UVV-CMP			2.5	
Third group	UHV-CMP		3		
Fourth group	UEV-CMP		3	2.5	

Table 6 Experimental conditions for model verification (MRR versus ultrasonic vibration)

Experiment	Polishing type	Polishing pressure/kPa	Horizontal ultrasonic amplitude/μm	Vertical ultrasonic amplitude/μm	Ultrasonic vibration frequency/kHz
First group	UVV-CMP	51.43		1, 2, 3, 4	35.3
Second group	UHV-CMP		1, 2, 3, 4		
Third group	UEV-CMP		1, 2, 3, 4	1, 2, 3, 4	
Fourth group	UVV-CMP			3	20.5, 25.1, 29.8 35.3, 39.9
Fifth group	UHV-CMP		3		
Sixth group	UEV-CMP		3	3	

Table 6. The polishing involves six groups of input variables according to ultrasonic vibration amplitude and frequency. The first three groups aim to verify the relation between MRR and vibration amplitude. The ultrasonic vibration amplitude varies from 1 to 4 μm by adjusting the output power of the ultrasonic generator. In the first three groups, the ultrasonic vibration frequency is kept constant at 35.3 kHz. The last three groups aim to verify the relation between MRR and vibration frequency. The ultrasonic vibration frequency varies from 20.5 to 39.9 kHz by designing different ultrasonic vibration devices as shown in Fig. 1 with different natural frequencies.

5.2 The relation between material removal rate and polishing pressure

Investigations are carried out for the comparison of conventional CMP with ultrasonic vibration-assisted CMP. The predicted relations between MRR and polishing pressure in the conventional CMP, UVV-CMP, UHV-CMP, and UEV-CMP processes are plotted in Fig. 19, respectively. It is known from these figures that MRR of conventional CMP increases approximately linearly with polishing pressure, and MRR of UHV-CMP, UVV-CMP, and UEV-CMP increases nonlinearly

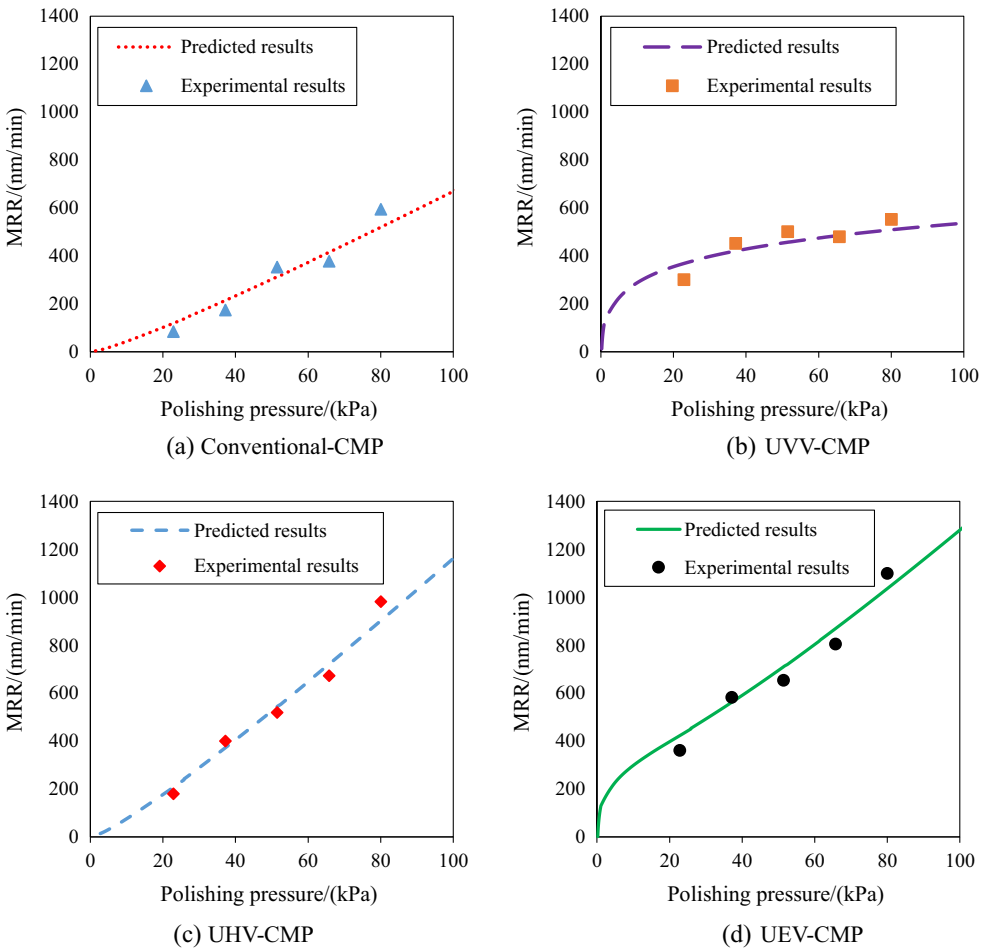

Fig. 19 The effect of polishing pressure on MRR. **a** Conventional-CMP, **b** UVV-CMP, **c** UHV-CMP, and **d** UEV-CMP

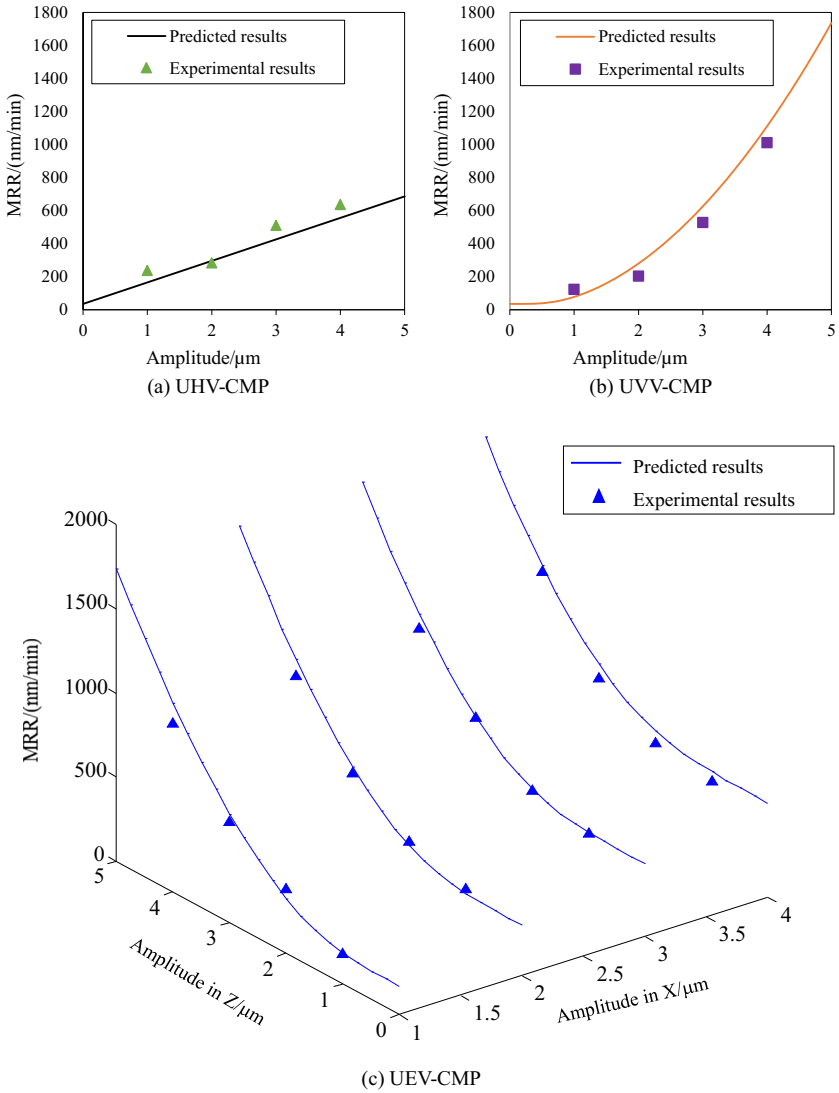

Fig. 20 The effect of ultrasonic vibration amplitude on MRR. **a** UHV-CMP, **b** UVV-CMP, and **c** UEV-CMP

with polishing pressure increases. However, one can observe that MRR of UVV-CMP varies slightly as polishing pressure when ultrasonic vibration characteristics are kept constant, and MRR of UHV-CMP varies significantly as polishing pressure when ultrasonic vibration characteristics keep constant. Hence, polishing pressure has significant effects on MRR in UVV-CMP of hard and brittle materials, while polishing pressure has less significant effects on MRR in UHV-CMP. Because UEV-CMP is combined by UHV-CMP and UVV-CMP, polishing pressure has significant effects on MRR in UEV-CMP of hard and brittle materials. The predicted MRRs from the model proposed in this paper and the experimental MRRs are also compared in Fig. 19. It can be seen from Fig. 19 that the predicted influences of input variable (polishing pressure) agree well with the trends determined experimentally. This set of experiments indicates that the polishing pressure is one of the main parameters affecting the MRR.

5.3 The relations between material removal rate and ultrasonic vibration

The effects of ultrasonic vibration amplitude and frequency on MRR are studied. As shown in Figs. 20 and 21, MRR in UHV-CMP, UVV-CMP, and UEV-CMP is influenced by the ultrasonic vibration amplitude and frequency. It can be seen from Figs. 20 and 21 that the MRR in UHV-CMP or UVV-CMP increases as the vibration amplitude and frequency increase. However, MRR increase in UVV-CMP due to the larger ultrasonic vibration amplitude and frequency is larger than that of UHV-CMP. The reasons for the efficient material removal in UVV-CMP lie in that abrasive indentation volume, which is significantly increased by ultrasonic vibration in vertical direction. Compared with the experimental MRR values, it can be seen that the trends of predicted influences of vibration amplitude and frequency agree well with the trends determined experimentally. The results from the material

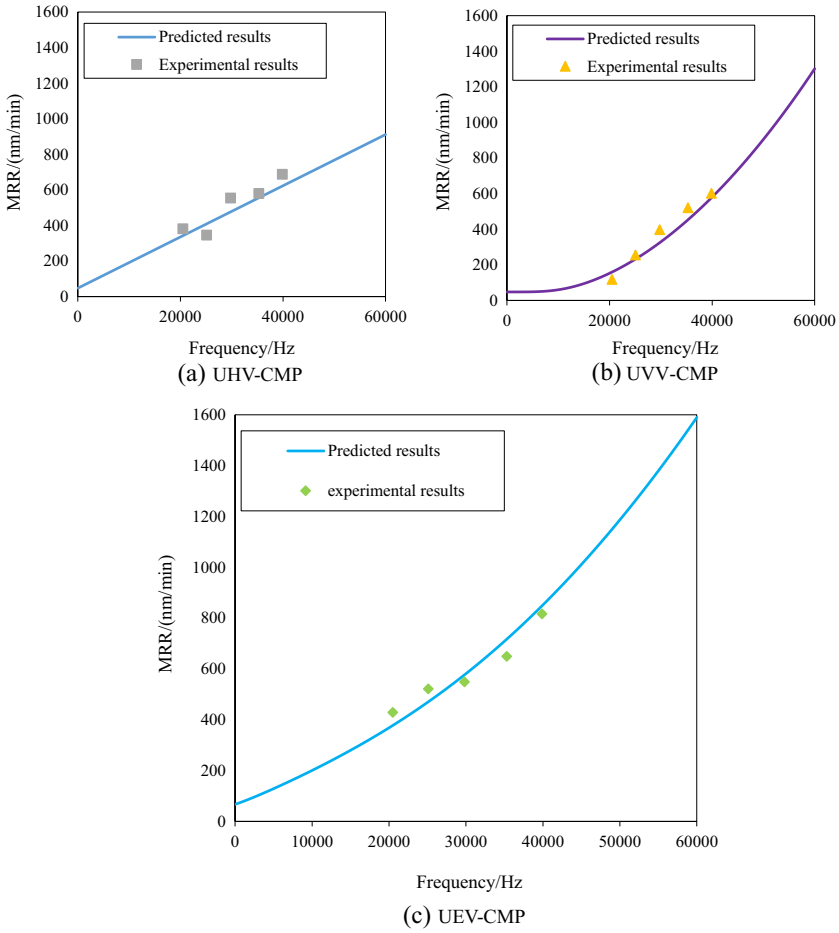

Fig. 21 The effect of ultrasonic vibration frequency on MRR. **a** UHV-CMP, **b** UVV-CMP, and **c** UEV-CMP

removal rate model and experiments show that the ultrasonic elliptical vibration can improve material removal by increasing vibration amplitude and frequency in vertical direction, while the horizontal vibration contributes less in increasing material removal rate.

6 Conclusions

The ultrasonic elliptical vibration is employed in combination with chemical mechanical polishing to finish hard and brittle materials, such as monocrystalline silicon. The material removal mechanism and the material removal rate model of ultrasonic elliptical vibration-assisted chemical mechanical polishing are proposed in order to interpret the probable reasons for the high polishing efficiency in material removal rate after the ultrasonic elliptical vibration is employed. Conclusions can be summarized as follows:

(1) UEV-CMP is able to improve the MRR and polished surface quality of hard and brittle material greatly compared with conventional CMP. The MRR of silicon samples polished by UEV-CMP is 693.6 nm/min, which is twice larger than that obtained by conventional CMP. The polished surface roughness value of UEV-CMP is 10.61 nm, which is much better than 27.61 nm obtained by conventional CMP. For UEV-CMP, a soft layer on workpiece surface formed by the chemical reaction of the slurry will be removed not only by the mechanical action of conventional CMP but also by the ultrasonic vibration action of UEV-CMP. The combined actions of ultrasonic elliptical vibration and conventional CMP can facilitate better polished surface and higher MRR.

(2) A physics-based material removal rate model for ultrasonic elliptical vibration-assisted chemical mechanical polishing of hard and brittle materials is developed. The model is used to predict the influences of input variables on MRR. These predicted influences are compared with those determined experimentally. The trends of predicted influences of input variables on MRR agree well with the trends determined experimentally.

(3) The MRR model shows that the actions of the ultrasonic elliptical vibration and the abrasive particles are the principal functions to remove the workpiece surface material. The effects of the ultrasonic elliptical vibration on the

interactions among the abrasive particles, polishing pad, and the workpiece are able to improve the MRR of UEV-CMP. The material of workpiece is removed by both of the micro-plowing and micro-indentation with the assistant of chemical effects during UEV-CMP. It indicates that such functions improved the material removal rate: the enhancement of the contact force between the abrasive particles and the workpiece surface, the impact of the abrasive particles to the workpiece surface, and the increase of the amplitude and frequency of the ultrasonic vibration.

Acknowledgements The authors would like to thank the National Natural Science Foundation of China (Grant 51275534) and Natural Science Foundation of Hunan Province, China (Grant 2015JJ2153) for their support to this work.

References

1. Qin K, Moudgil B, Park CW (2004) A chemical mechanical polishing model incorporating both the chemical and mechanical effects. Thin Sold Films 446:277–286
2. Lee HS, Jeong HD (2009) Chemical and mechanical balance in polishing of electronic materials for defect-free surfaces. CIRP Ann Manuf Technol 58:485–490
3. Zhong ZW, Tian YB, Ang YJ, Wu H (2012) Optimization of the chemical mechanical polishing process for optical silicon substrates. Int J Adv Manuf Technol 60:1197–1206
4. Lei H, Tong KY, Wang ZY (2016) Preparation of Ce-doped colloidal SiO_2 composite abrasives and their chemical mechanical polishing behavior on sapphire substrates. Mater Chem Phys 172: 26–31
5. Zhang ZF, Yu L, Liu WL, Song ZT (2010) Surface modification of ceria nanoparticles and their chemical mechanical polishing behavior on glass substrate. Appl Surf Sci 256:3856–3861
6. Tian YB, Zhong ZW, Lai ST, Ang YJ (2013) Development of fixed abrasive chemical mechanical polishing process for glass disk substrates. Int J Adv Manuf Technol 68:993–1000
7. Gong H, Pan GS, Zhou Y, Shi XL, Zou CL, Zhang SM (2015) Investigation on the surface characterization of Ga-faced GaN after chemical-mechanical polishing. Appl Surf Sci 338:85–91
8. Zhou Y, Pan GS, Shi XL, Zhang SM, Gong H, Luo GH (2015) Effects of ultra-smooth surface atomic step morphology on chemical mechanical polishing (CMP) performances of sapphire and SiC wafers. Tribol Int 87:145–150
9. Hu XK, Song ZT, Pan ZC, Liu WL, Wu LC (2009) Planarization machining of sapphire wafers with boron carbide and colloidal silica as abrasives. Appl Surf Sci 255:8230–8234
10. Xu L, Zou CL, Shi XL, Pan GS, Luo GH, Zhou Y (2015) Fe-N_x/C assisted chemical–mechanical polishing for improving the removal rate of sapphire. Appl Surf Sci 343:115–120
11. Pei ZJ, Ferreira PM (1998) Modeling of ductile-mode material removal in rotary ultrasonic machining. Int J Mach Tools Manuf 38: 1399–1418
12. Brehl DE, Dow TA (2008) Review of vibration-assisted machining. Precis Eng 32:153–172
13. Xu WH, Lu XC, Pan GS, Lei YZ, Luo JB (2010) Ultrasonic flexural vibration assisted chemical mechanical polishing for sapphire substrate. Appl Surf Sci 256:3936–3940
14. Xu WH, Lu XC, Pan GS, Lei YZ, Luo JB (2011) Effects of the ultrasonic flexural vibration on the interaction between the abrasive particles; pad and sapphire substrate during chemical mechanical polishing (CMP). Appl Surf Sci 257:2905–2911
15. Tsai MY, Yang WZ (2012) Combined ultrasonic vibration and chemical mechanical polishing of copper substrates. Int J Mach Tools Manuf 53:69–76
16. Li L, He Q, Zheng M, Liu Z (2015) Contribution of ultrasonic traveling wave to chemical-mechanical polishing. Ultrasonics 56: 530–538
17. Zhao QL, Sun ZY, Guo B (2016) Material removal mechanism in ultrasonic vibration assisted polishing of micro cylindrical surface on SiC. Int J Mach Tools Manuf 103:28–39
18. Li YG, Wu YB, Zhou LB, Fujimoto M (2014) Vibration-assisted dry polishing of fused silica using a fixed-abrasive polisher. Int J Mach Tools Manuf 77:93–102
19. Yang WP, Xu JW, Wu YB (2008) Chemical-mechanical polishing principle and experimental system of ultrasonic elliptic vibration. J Nanjing Univ Aeronaut Astronaut 40(6):753–757 (in Chinese)
20. Liang ZQ, Wu YB, Wang XB, Zhao WX (2010) A new two-dimensional ultrasonic assisted grinding (2D-UAG) method and its fundamental performance in monocrystal silicon machining. Int J Mach Tools Manuf 50:728–736
21. Suzuki H, Hamada S, Okino T, Kondo M, Yamagata Y, Higuchi T (2010) Ultraprecision finishing of micro-aspheric surface by ultrasonic two-axis vibration assisted polishing. CIRP Ann-Manuf Technol 59:247–350
22. Yang WP, Wu YB, Yang HF (2011) Mechanism and experimental investigation on silicon wafer hybrid polishing by ultrasonic-elliptic-vibration chemical-mechanical. Adv Mater Res 314-316: 829–836
23. Haynes WM (2014) CRC handbook of chemistry and physics. CRC press, London
24. Engel PA (1976) Impact wear of materials. Elsevier Scientific Pub. Co, New York
25. Bhushan B (2013) Introduction to tribology. John Wiley and Sons, London
26. Hu Q, Liu DF, Zou WB (2014) Material removal model and experimental analysis in the CMP of si-based fiber array. Adv Mater Res 941-944:2345–2365
27. Jiang JZ, Zhao YW, Wang YG, Luo JB (2008) A chemical mechanical polishing model based on the viscous flow of the amorphous layer. Wear 265:992–998
28. Luo JF, Dornfeld DA (2001) Material removal mechanism in chemical mechanical polishing: theory and modeling. IEEE Trans Semicond Manuf 14(2):112–133
29. Jeng YR, Huang PY (2005) A material removal rate model considering interfacial micro-contact wear behavior for chemical mechanical polishing. Trans ASME-J Tribol 127:190–197
30. Zhao YW, Chang L (2002) A micro-contact and wear model for chemical-mechanical polishing of silicon wafers. Wear 252:220–226